

CHROM. 21 908

DETERMINATION OF DIFFUSION COEFFICIENTS OF PROTEINS IN BEADED AGAROSE BY GEL FILTRATION

P. A. DAVIES

Medical Engineering Unit, Department of Engineering Science, University of Oxford, 43 Banbury Road, Oxford OX2 6PE (U.K.)

(First received April 25th, 1989; revised manuscript received July 26th, 1989)

SUMMARY

A method for determining approximately the coefficient of diffusion of solute molecules in beaded gels, based on the analysis of breakthrough curves obtained in gel filtration, is described. This is applied to the diffusion of porcine serum proteins, gamma-globulin and fibrinogen in Sepharose CL-4B. The diffusion coefficients at 20°C are 11.2 and 3.6 $\mu\text{m}^2/\text{s}$, respectively, about half those calculated from the partition coefficients using published equations.

INTRODUCTION

The problem of calculating breakthrough curves in beds of porous spherical particles was originally treated by Rosen^{1,2}, who used a Laplace transform method. Subsequent workers have presented improved methods of inverting the Laplace transform^{3–5} and solved more complicated problems of breakthrough curve prediction^{6–8}. The aim here was to use experimental breakthrough curves to calculate the diffusion coefficients, D_s , of solutes in the spherical particles of a gel filtration column. Such coefficients could be of interest in the design of gel-filtration operations, in the theory of electrophoresis and in the study of affinity chromatography, in which it has been suggested that bulk diffusion can limit the performance⁹.

The breakthrough curve follows a step change in concentration at the column inlet. It is essentially an integrated form of the peak produced as a result of the injection of a sudden pulse of solute at the column inlet, as is used, for example, in elution chromatography. One approach to evaluating mass-transfer parameters, such as D_s , is to study the moments of this peak, which may be related to these parameters by analytical expressions¹⁰. In order for D_s to become the dominant parameter in determining the shape of the peak, however, it is desirable to use a residence time that is smaller than the time scale of diffusion in and out of the stationary phase. Also, the system must be such that, at equilibrium, a substantial fraction of the solute is distributed inside the stationary phase. Under these conditions, the peak shows very long tailing, giving rise to a significant experimental difficulty in measuring moments¹¹ (and hence also in determining the variance and theoretical plate height) as these

measurements become very sensitive to baseline errors at large times, and it becomes difficult to know when to truncate the calculations. Simple methods of measuring variance, based, for example, on the width of the peak at half-height, or on baseline intercepts¹², may no longer be accurate because they assume the peak to be Gaussian.

To overcome this problem, De Lasa *et al.*¹³ suggested the use of a longer, pulse input to the column, and put forward an analysis that enables the length of the pulse to be chosen in such a way that the effect of detector error is minimized, enabling the method of moments to be applied with greater accuracy. An alternative to the method of moments is to compare experimental and theoretical responses to pulse inputs after transformation into the frequency domain^{14,15}. It is also possible to use harmonic variations in concentrations as the input, and to compare the attenuation and phase lag at various frequencies with theoretical predictions^{16,17}, although a drawback is that a special waveform generator is required.

In this work, experimental and theoretical breakthrough curves are matched on the basis of the area A beneath the curve up the point where the dimensionless time (based on the mean residence time) equals unity. This area has been referred to as the holdback by Dankwerts¹⁸. An important requirement is to ensure that D_s is the main parameter affecting A , and if necessary to correct for the smaller effects of other parameters.

THEORY

The degree of chemical interaction between the purified form of agarose used in these experiments (Sephacrose CL-4B) and most proteins is reported to be very small¹⁹, and the results of the experiments to be described here tend to confirm this for the proteins studied. Terms representing chemical adsorption are therefore omitted from the analysis. The structure of agarose is very fine. It is thought to consist of a matrix of fibres of approximate diameter 5 nm^{20,21}, whereas the particles used here have a diameter of the order of 100 μm . It is proposed, therefore, to treat the interior of each particle as a homogeneous continuum. The object is to find the diffusion coefficients, D_s , of proteins inside this continuum. The model equations are as follows: in the mobile phase, *i.e.*, outside the particles:

$$\frac{\partial c_m}{\partial t} + u \cdot \frac{\partial c_m}{\partial x} = D_L \cdot \frac{\partial^2 c_m}{\partial x^2} - SD_s \cdot \left. \frac{\partial c_s}{\partial r} \right|_{r=R} \quad (1)$$

in the stationary phase, *i.e.*, inside the particles, which are spheres:

$$\frac{\partial c_s}{\partial t} = D_s \cdot \frac{\partial c_s}{\partial r} + \frac{2}{r} \cdot \frac{\partial^2 c_s}{\partial r^2} \quad (2)$$

subject to the following boundary conditions:

$$\begin{aligned} c_m(x, 0) &= c_0 \\ c_s(x, r, 0) &= K_{av}c_0 \\ c_m(0, t > 0) &= c_{in} \\ k(c_m - c_s/K_{av}) &= -D_s \cdot \left. \frac{\partial c_s}{\partial r} \right|_{r=R} \end{aligned} \quad (3)$$

where c_m and c_s are the concentrations in the mobile and stationary phases, respectively, c_0 is the initial concentration in the mobile phase, c_{in} the concentration introduced at the inlet at time $t = 0$, x is the distance along the column axis measured from the inlet, r is the radial coordinate inside the spherical particles, of radius R , of the stationary phase, u is the average velocity based on the volume of the mobile phase, S is the surface area per unit volume of mobile fluid, D_L is a coefficient of longitudinal dispersion in the mobile phase, K_{av} is the partition coefficient and k is the coefficient of surface mass transfer.

The inclusion of the longitudinal dispersion term means that the processes taking place in the column are not theoretically independent of events downstream of the column outlet. Although in practice such a dependence is likely to be very small, in order for the mathematical description to be complete it is necessary to introduce a downstream boundary condition. A convenient assumption is

$$c_m(\infty, t) = 0 \quad (4)$$

Non-dimensionalized quantities are introduced as follows: dimensionless time $t^* = [V(t) - V_m]/V_a$, where $V(t)$ is the volume discharged from the column after time t , V_m the volume of the mobile phase and V_a the partial volume inside the stationary phase, which may be considered accessible to the solute molecules (these volumes are explained in Fig. 1); dimensionless outlet concentration

$$y(t^*) = [c_{out} - c_0]/[c_1 - c_0] \quad (5)$$

where c_{out} is the measured outlet concentration (hence y is initially zero and increases to one); a dimensionless diffusion coefficient

$$D^* = D_s V_a / R^2 Q \quad (6)$$

where Q is the discharge from the column; and a dimensionless surface mass transfer resistance

$$\alpha = D_s K_{av} / k R \quad (7)$$

Application of the Laplace transform leads to an ordinary second-order differential equation, from which the solution for the outlet concentration $y(t^*)$ may be obtained in terms of an inverse Laplace transform (e.g., see ref. 8). When D_L/uL is small (where L is the length of the column), an appropriate form is

$$y(t^*) = \mathcal{L}^{-1} \left\{ \frac{1}{s} \exp(-\varphi(s) + (D_L/uL) [V_m/V_a + \varphi(s)]^2) \right\} \quad (8)$$

where

$$\varphi(s) = 3D^* \cdot \frac{\sqrt{s/D^*} \coth \sqrt{s/D^*} - 1}{1 + \alpha(\sqrt{s/D^*} \coth \sqrt{s/D^*} - 1)}$$

s being the transform variable.

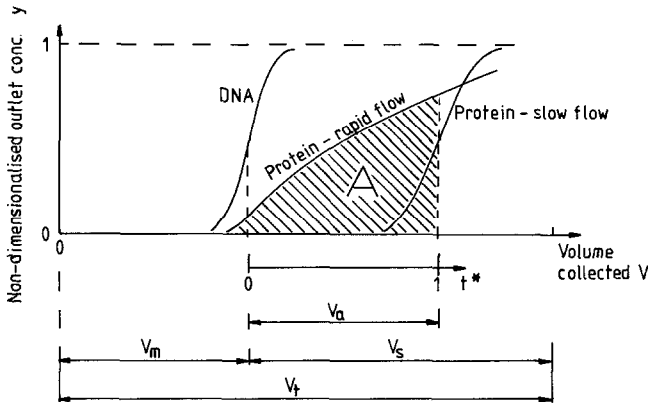


Fig. 1. Sketch of breakthrough curves giving explanation of the volumes referred to in the text. Molecules such as DNA, which are too large to penetrate the stationary phase, reach the outlet once a volume of fluid equal to the volume V_m of the mobile phase has been discharged. Smaller molecules, such as proteins, can penetrate a certain volume V_a of the stationary phase. The non-dimensionalized time scale t^* is shown.

As the solutions published by Rosen² did not cover a sufficient number of values of D^* for the present purpose, and did not account for the effect of the longitudinal dispersion coefficient D_L , a means of calculating this inverse transform was needed. The Numerical Algorithms Group Fortran library routine C06LAF (ref. 22) was used. A note on the computation is given in the Appendix. The solutions agreed well with those of Rosen² in the cases where comparisons were possible. The above choice of non-dimensionalizing time scale was found to be convenient in obtaining solutions over widely varying values of D^* .

In order to match the theoretical and experimental curves, the parameter used was the area A beneath the normalized breakthrough curve as illustrated in Fig. 1. A is defined as

$$A = \int_{-\infty}^1 y(t^*) dt^* \quad (9)$$

When D^* is large and α is small, the breakthrough is considerably delayed by diffusion into the stationary phase and A tends towards zero, but when D^* is small (or α is very large) the flow is too rapid for diffusion to occur and A tends towards one. From the above equations, A appears to depend on four parameters, *i.e.*, $A(D^*, \alpha, D_L/uL, V_m/V_a)$. At the computational stage, however, it was found that, for the small values of D_L/uL of interest, A was almost independent of D_L/uL and of V_m/V_a provided that the product of these two was kept constant (see Table I). The number of parameters was therefore effectively reduced to three. Fig. 2 shows the variation of A with D^* for different values of D_L/uL , with $\alpha = 0$ and $V_m/V_a = 1$, since this value was appropriate to the experiments presented here. When the distribution ratio V_m/V_a differs significantly from one, the contour variable in Fig. 2 may be interpreted as $(V_m/V_a)(D_L/uL)$.

TABLE I

COMPUTED VALUES OF A , WITH $\alpha = 0$, SHOWING THAT A IS APPROXIMATELY CONSTANT IF $(V_m/V_a)(D_L/uL)$ AND D^* ARE CONSTANT

D^*	A			
	$D_L/uL = 0$	$D_L/uL = 0.02,$ $V_m/V_a = 0.5$	$D_L/uL = 0.01,$ $V_m/V_a = 1$	$D_L/uL = 0.005,$ $V_m/V_a = 2$
0.03	0.589	0.600	0.600	0.601
0.05	0.406	0.424	0.422	0.424
0.10	0.511	0.526	0.527	0.527

When $D_L/uL = 0$, the choice of V_m/V_a becomes irrelevant and the resulting dependence of A on D^* is shown in Fig. 3 for four different values of α . Given a measurement of A and estimates of α , D_L/uL and V_m/V_a , Figs. 2 and 3 can be used to determine D^* , and hence D_s , without the need to repeat the computations of breakthrough curves. An attraction of matching A , rather than some other parameter describing the curves, is that random experimental and computational errors tend to be averaged out in the process of integration. In order to obtain reasonable accuracy, the flow-rate should be chosen so that A is between 0.4 and 0.8. If it is assumed that A can be assessed with a fixed absolute accuracy, the optimum value is about 0.5.

The surface mass-transfer resistance α may be estimated on the basis of Pfeffer's model^{23,24}. This model treats the spheres as if they were each enclosed in a concentric,

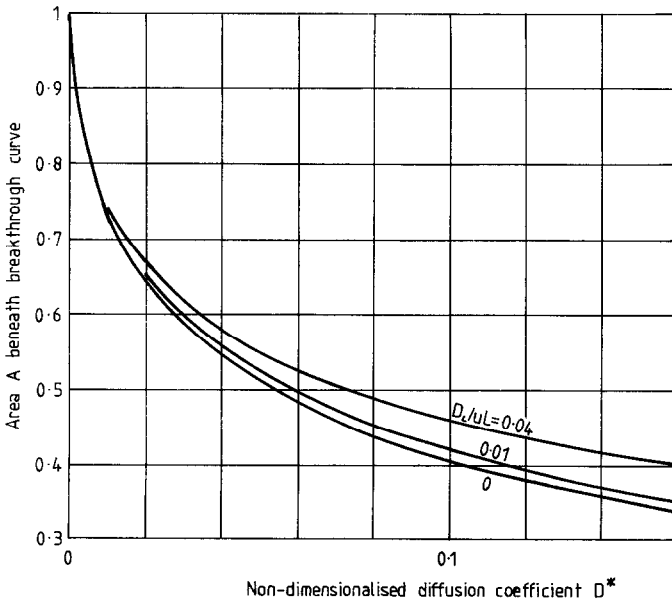


Fig. 2. Theoretical area A beneath the breakthrough curves, plotted against D^* for three values of D_L/uL . $\alpha = 0$, $V_m/V_a = 1$.

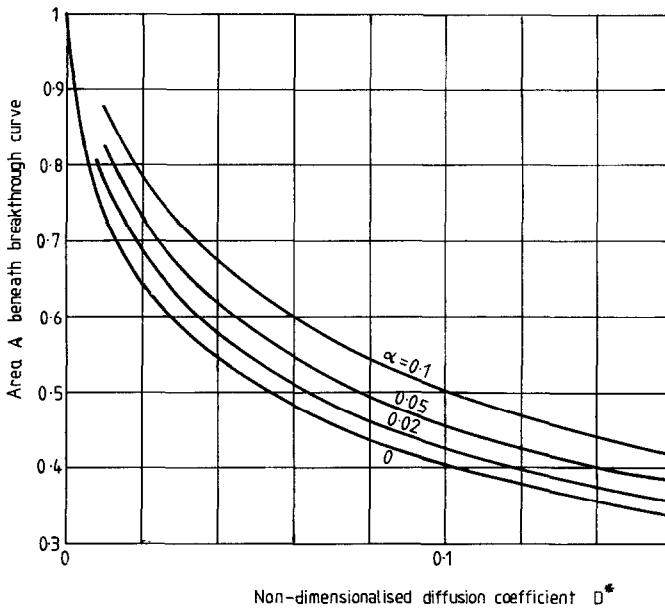


Fig. 3. Theoretical area A beneath the breakthrough curves, plotted against D^* for four values of α . $D_L/uL = 0$.

spherical fluid envelope, the radius of which is chosen so that the total volume of fluid in the envelopes is the same as that contained in the mobile phase of the real column. The solutions for the mass-transfer coefficient are based on the assumption of creeping flow (*i.e.*, low Reynolds number) and at high reduced velocities the model gives the following correlation (in a slightly rearranged form), which agrees well with experimental studies²⁴:

$$Sh = Bv^{1/3} \quad (10)$$

where the Sherwood number $Sh = Rk/D_m$, the reduced velocity $v = 2Ru/D_m$ (D_m is the coefficient of diffusion in the mobile phase) and the dimensionless constant B is a function of the ratio γ of the sphere diameter to that of the envelope:

$$B = 0.63 \left[\frac{(1 - \gamma^5)(1 - \gamma^3)}{2 - 3\gamma + 3\gamma^5 - 2\gamma^6} \right]^{1/3} \quad (11)$$

and hence of the bed voidage, since $V_m/V_t = 1 - \gamma^3$. For a gel filtration column, V_m/V_t is typically about 1/3, giving $B = 1.35$.

The coefficient of longitudinal dispersion in the mobile phase, D_L in eqn. 1, can be thought of as describing the dispersion which would occur if the solute were not able to enter the stationary phase. Such dispersion results from the inequality of residence times along various streamlines in the mobile phase (it is assumed that the flow is laminar, as the Reynolds number based on particle diameter is less than 0.2 in these

studies), and is reduced by the tendency for molecules to diffuse across the streamlines. This type of dispersion has been referred to as "eddy diffusion"^{25,26}, although it is, of course, a result of convection. Pure longitudinal diffusion, which would occur even if there were no flow in the column, is likely to be negligible in the experiments described here. The form of the longitudinal dispersion term in eqn. 1 is, however, analogous to a diffusive term, and this has an empirical justification as the Gaussian residence time distribution which it predicts is often observed in practice. Insofar as the interstices in a bed of particles can be compared to a tangled bundle of intermingling, narrow tubes, the model has also a theoretical basis in Taylor's analysis of dispersion in pipe flow²⁷. The complex geometry of packed columns is such that D_L cannot be predicted precisely. Practical correlations have to rely on some empirically determined factors that depend on the structure of the bed^{28,31}. The correlation of Horváth and Lin³¹ gives for example (with longitudinal diffusion neglected):

$$h = \frac{2\lambda}{1 + \omega v^{-1/3}} \quad (12)$$

where h is the reduced theoretical plate height, defined as

$$h = \frac{L}{2R} \cdot \frac{\sigma^2}{V_m^2} \quad (13)$$

σ being the standard deviation of a chromatographic peak, plotted on a volume axis. The empirical constants λ and ω were given values of 10.47 and 11.2, respectively, in experiments with columns of glass beads³¹. This model can be used to estimate longitudinal dispersion in the mobile phase, since³²

$$\frac{D_L}{uL} = \frac{1}{2} \cdot \frac{\sigma^2}{V_m^2} \quad (14)$$

In view of the likely variations from one column to another, however, a preliminary experiment was performed to estimate D_L using a column that was as similar as possible to that in the main experiments, but with a packing that the solute could not penetrate.

EXPERIMENTAL

Preliminary experiment: estimation of D_L

The object of this experiment was to study the dispersion of a solute that was excluded from the stationary phase. The conditions and method were, as far as possible, the same as those used in the main experiment described below. A 3.1-cm high bed of Sephadex G-25 150 (Pharmacia) with spheres of average diameter 110 μm was used instead of the Sepharose CL-4B. The solute and solvent were porcine γ -globulin (2 mg/ml) and phosphate-buffered saline (pH 7.2), respectively, and the flow-rate varied from 1 to 20 ml/min. The breakthrough curve was differentiated automatically

by the spectrophotometer, giving nearly symmetrical peaks. The height of this peak gave the maximum slope, dy/dV , of the breakthrough curve. From the properties of the (assumed) Gaussian residence time distribution, the dimensionless variance was calculated as

$$\frac{\sigma^2}{V_m^2} = \frac{1}{2 \pi V_m^2 (dy/dV)^2} \quad (15)$$

and hence h from eqn. 13. As a check, the values of h were also calculated on the basis of the widths of the peaks.

Mean experiment: measurement of A

The gel filtration medium was Sepharose CL-4B cross-linked 4% agarose beads (Pharmacia-LKB). The object was to measure the area A (and hence estimate D_s) for two different proteins, porcine γ -globulin (Sigma G2512) and porcine fibrinogen (Sigma F2629), in the Sepharose. These proteins were made up at concentrations of 2 mg/cm^3 in phosphate-buffered saline (pH 7.2) and prefiltered through $0.45\text{-}\mu\text{m}$ membrane filters. To measure the breakthrough curves, and hence estimate diffusion coefficients, the column shown in Fig. 4 was devised. It had an inside diameter of 1.45 cm and the bed height was between 2.8 and 3.0 cm. The top space above the column could be completely washed out with a new fluid before this fluid was introduced into the column. A sharp, step change in concentration was therefore obtained at the inlet. The dead space downstream of the column, including the optical cell and connecting tubing, totalled 0.1 ml. Liquid was supplied from a Watson-Marlow 501U roller pump. Discharge, which varied from 2.78 to 8.58 ml/min, was calculated from the time taken to collect 5 ml at the outlet. The absorbance of the outlet fluid was monitored at 280 nm using a Shimadzu UV-160 spectrophotometer. A flow cell was constructed having an optical path length of 1.5 mm. V_m was measured by the exclusion of DNA, the source of which was salmon testes (Pharmacia 27-4576-01) or calf thymus (Sigma D-1501). To find $V_m + V_a$ (and hence V_a), the column was saturated with protein solution of known absorbance and then eluted with a known volume of buffer. $V_m + V_a$ was then calculated from the absorbance of the eluted solution.

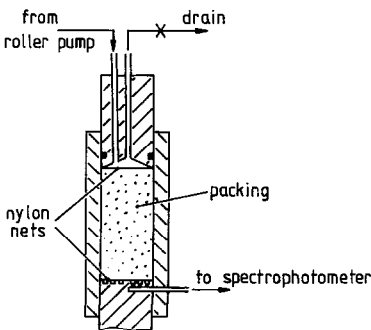


Fig. 4. Column used for measuring breakthrough curves.

These Sepharose CL-4B particles were spherical and had a mean diameter \pm standard deviation of $80 \pm 20 \mu\text{m}$, based on the microscopic examination of 100 beads.

In some experiments the column initially contained no protein (*i.e.*, $c_0 = 0$) before protein solution was introduced at the inlet. In others, the column was initially filled with a uniform concentration of protein solution ($c_0 = 2 \text{ mg/ml}$), and zero concentration was introduced at the inlet.

Experiments were carried out at between 18 and 21°C.

RESULTS

The spectrophotometer printed out values of absorbance against time and these were converted into graphs of y against t^* , with allowance made for the 0.1-ml dead volume of the optical cell and tubing. At the same flow-rates, curves obtained with $c_0 = 0$ and 2 mg/cm^3 were similar when presented in this way, indicating that there was not a significant chemical interaction between the proteins and the Sepharose. In order to calculate A , the graphs were divided into about eight strips and Simpson's rule was applied. The results are shown in Tables II and III. A was used to obtain D^* from Fig. 2. Initially it was assumed that both α and D_L were zero.

From D^* , D_s could be calculated on the basis of eqn. 6, given the radius R of the particles. Whereas the theoretical model assumes them to be of uniform size, in reality they are not. However, the work of Rasmuson⁷ has shown that, when the particle-size distribution is as narrow as in this instance, the breakthrough curve is very little affected. The appropriate average radius to use is that giving an equivalent surface area per unit volume of the particles⁸, *i.e.*,

$$\bar{R} = \frac{\sum R^3}{\sum R^2} = 43 \mu\text{m} \quad (n = 100) \quad (16)$$

The mean values of D_s obtained were $9.9 \mu\text{m}^2/\text{s}$ for porcine γ -globulin and $3.2 \mu\text{m}^2/\text{s}$ for porcine fibrinogen, but this was before making any correction for the surface mass-transfer resistance, α , and longitudinal dispersion in the mobile phase, D_L/uL .

To correct for α , it was assumed still that $D_L/uL = 0$, and k was estimated on the basis of Pfeffer's model (eqns. 10 and 11), using for D_m published values for similar proteins in free solution (see Discussion). It was necessary to know D_s before α could be calculated, whereas of course the corrected value of D_s was not yet determined. Initially α was calculated as on the basis of the uncorrected value of D_s . A new value of D_s was then determined from Fig. 3, using linear interpolation between the contours. Once the value of D_s corrected for both D_L and α had been found as described below, it was then possible to iterate to obtain new values of α and D_s , but in fact such iteration altered the result by only a very small amount.

Fig. 5 shows the result of the preliminary experiment in the form of a plot of reduced theoretical plate height, h , against reduced velocity, v . The following linear regression was obtained:

$$h = 2.0 + 4.1 \cdot 10^{-4}v \quad (17)$$

TABLE II
RESULTS WITH PORCINE γ -GLOBULINS

Column, $2.8 \text{ cm} \times 1.45 \text{ cm I.D.}$ $V_1 = 4.62 \text{ cm}^3$, $V_m = 1.67 \text{ cm}^3$ (DNA from salmon testes), $V_a = 1.84 \text{ cm}^3$, $K_{av} = 0.62$, $\bar{R} = 43 \text{ } \mu\text{m}$, $D_m = 40 \text{ } \mu\text{m}^2/\text{s}$, $B = 1.3$.

Run	Q (ml/min)	ν (10^3)	A (measured)	$\alpha = 0, D_L/\mu L = 0$		α from Pfeffer, $D_L/\mu L = 0$		$\alpha = 0, D_L/\mu L$ from eqn. 17		Corrected D_s ($\mu\text{m}^2/\text{s}$)	
				D^* (Fig. 2)	D_s ($\mu\text{m}^2/\text{s}$)	α	D^* (Fig. 3)	D_s ($\mu\text{m}^2/\text{s}$)	$D_L/\mu L$		D^* (Fig. 2)
<i>(i) $c_0 = 0, c_{in} = 2 \text{ mg/cm}^3$:</i>											
1	8.58	5.15	0.477	0.063	9.1	0.007	0.067	0.006	0.066	9.5	10.0
2	6.36	3.82	0.415	0.094	10.0	0.009	0.100	0.005	0.099	10.9	11.5
<i>(ii) $c_0 = 2 \text{ mg/cm}^3, c_{in} = 0$:</i>											
3	8.58	5.15	0.459	0.070	10.1	0.008	0.075	0.006	0.074	10.6	11.3
4	6.36	3.82	0.411	0.097	10.3	0.009	0.104	0.005	0.102	10.9	11.8
Mean \pm standard deviation										11.2 \pm 0.8	

TABLE III
RESULTS WITH PORCINE FIBRINOGEN

Column, 3.0 cm \times 1.45 cm I.D. $V_1 = 4.95 \text{ cm}^3$, $V_m = 1.49 \text{ cm}^3$ (DNA from calf thymus), $V_a = 1.36 \text{ cm}^3$, $K_{av} = 0.39$, $\bar{R} = 43 \text{ }\mu\text{m}$, $D_m = 19.7 \text{ }\mu\text{m}^2/\text{s}$, $B = 1.4$.

Run	Q (ml/min)	v (10^3)	A (measured)	$\alpha = 0, D_L/\mu\text{L} = 0$		α from Pfeffer, $D_L/\mu\text{L} = 0$		$\alpha = 0, D_L/\mu\text{L}$ from eqn. 17		Corrected D_s ($\mu\text{m}^2/\text{s}$)
				D^* (Fig. 2) ($\mu\text{m}^2/\text{s}$)	D_s ($\mu\text{m}^2/\text{s}$)	α	D^* (Fig. 3) ($\mu\text{m}^2/\text{s}$)	D_s ($\mu\text{m}^2/\text{s}$)	$D_L/\mu\text{L}$	
(i) $c_0 = 0, c_{in} = 2 \text{ mg/cm}^3$:										
5	6.98	10.2	0.617	0.024	3.8	0.003	0.025	0.009	0.027	4.3
6	4.76	6.97	0.595	0.028	3.0	0.002	0.029	0.007	0.030	3.2
7	2.78	4.07	0.505	0.053	3.3	0.003	0.055	0.005	0.056	3.5
(ii) $c_0 = 2 \text{ mg/cm}^3, c_{in} = 0$:										
8	6.98	10.2	0.640	0.021	3.3	0.002	0.021	0.009	0.022	3.5
9	4.76	6.97	0.600	0.027	2.9	0.002	0.028	0.007	0.029	3.1
10	2.78	4.07	0.516	0.049	3.1	0.003	0.051	0.005	0.052	3.3
Mean \pm standard deviation										3.6 \pm 0.5

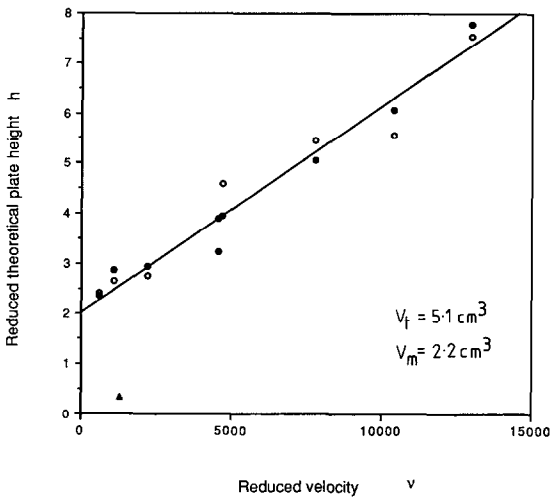


Fig. 5. Reduced theoretical plate height h versus reduced velocity v , in preliminary experiment using Sephadex G-25 150 and porcine γ -globulin, from peaks obtained by differentiation of breakthrough curves: ○ = from peak height; ● = from peak width at half height. ▲ = Value calculated from the height of the peak when the packing was removed and the column volume reduced to zero.

Free-solution diffusion coefficients (see Discussion) were used to calculate v . The correlation of Horváth and Lin³¹ predicts larger values of h . To estimate D_L/uL for the main experiment, eqn. 17 was used because (by eqns. 13 and 14) $D_L/uL = hR/L$. On the basis of Fig. 2, values of D_s corrected for D_L/uL were calculated as shown in Tables II and III. For this purpose it was assumed that $\alpha = 0$.

The above corrections for α and D_L/uL were made separately, *i.e.* assuming the other to be zero in each instance. As these corrections were small, it was reasonable to regard them as being additive, giving $D_s = 11.2 \mu\text{m}^2/\text{s}$ (γ -globulin) and $3.6 \mu\text{m}^2/\text{s}$ (fibrinogen). To have tried to make the corrections simultaneously would have been very tedious, as a large number of curves of A against D^* , each corresponding to a different combination of α and D_L/uL , would have had to have been calculated. The

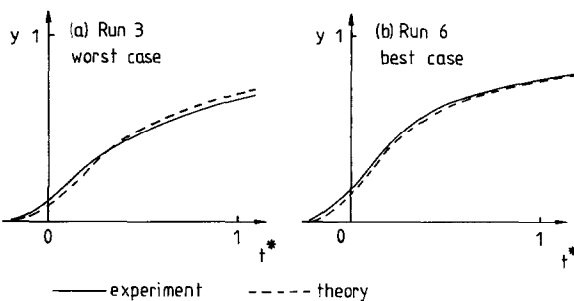


Fig. 6. Comparison of experimental (solid lines) and theoretical (dashed lines) breakthrough curves in (a) the worst case and (b) the best case.

final values of D_s , α and D_L/uL determined for each run, when fed back into the computer, gave values of A that agreed to within about 1% with the measured values. This showed the method of adding the corrections to be satisfactory.

Fig. 6 shows the agreement between the theoretical curves (calculated using the mean values of D_s for each protein) and experimental curves in what were judged to be the best and worst cases.

DISCUSSION

The corrections for surface mass-transfer resistance, α , and longitudinal dispersion in the mobile phase, D_L were small, giving together an increase of 13% in the estimated values of D_s , probably only just significant given the experimental accuracy in measuring A . The fact that the resistance to mass transfer in the mobile phase is only a small part of the total resistance is, perhaps, not surprising considering that the mobile phase occupies only about one third of the total column volume, that transfer is aided by convection and that the diffusivity is greater than in the stationary phase as there are no obstructions. Relatively low surface mass-transfer resistance has also been reported in the low-Reynolds-number flow of hydrocarbon gases through silica gel packed columns³³.

The estimation of D_L in the preliminary experiment could not be exact as the column was similar to but not identical with that of the main experiment. However, as the correction for D_L was small, even fairly large errors would not have a great effect on the final result.

As this method of determining diffusion coefficients is indirect, it is limited in accuracy, but it is thought that with care it should generally be possible to obtain values that are accurate to within about $\pm 25\%$. It is particularly important to measure V_m as accurately as possible. Light scattering, as an alternative means of measuring diffusion coefficients, would probably be difficult to apply owing to scattering of light by the Sepharose particles.

In order to use the present method, the residence time in the mobile phase must be sufficiently small compared with the diffusion time in the stationary phase. However, as flow-rate is limited by compaction of the Sepharose, this is difficult to achieve with molecules that diffuse much more rapidly than the γ -globulin molecules studied here. This could be overcome by using larger particles, which would increase the diffusion time and decrease the resistance to flow, but such particles are not so readily available commercially.

It is interesting to compare the diffusion coefficients inside the Sepharose particles, D_s , with those in free solution, D_0 . Values for D_0 have been reported for human serum proteins³⁴: $40 \mu\text{m}^2/\text{s}$ for immunoglobulin-G (the main constituent of the γ -globulin fraction) and $19.7 \mu\text{m}^2/\text{s}$ for fibrinogen. It seems probable that similar values would apply in the pig. Ogston *et al.*³⁵ derived the following equations from theoretical considerations of molecular motion inside a fibre matrix:

$$\begin{aligned} D_s/D_0 &= \exp[-(r_s + r_f)v_f^{1/2}/r_f] \\ K_{av} &= \exp[-(r_s + r_f)^2 v_f/r_f^2] \end{aligned} \quad (18)$$

TABLE IV

COMPARISON OF EXPERIMENTALLY DETERMINED DIFFUSION COEFFICIENTS WITH VALUES GIVEN BY THEORY OF OGSTON *ET AL.*³⁵

<i>Protein</i>	K_{av} (<i>experiment</i>)	D_s/D_0 (<i>experiment</i>)	D_s/D_0 (<i>theory</i>)
γ -Globulin	0.62	0.28	0.50
Fibrinogen	0.39	0.18	0.37

where r_s and r_f are the radii of the solute molecules and fibres, respectively, and v_f is the volume of fibres per total volume. From these equations it follows that

$$D_s/D_0 = \exp[-\sqrt{(-\ln K_{av})}] \quad (19)$$

It can be seen in Table IV that the experimental values of D_s/D_0 are about half of the theoretical values based on the experimental values of K_{av} (calculated as $K_{av} = V_a/V_s$). As the theory of Ogston *et al.*³⁵ was derived for spherical molecules, in principle it should be more applicable to the γ -globulin than to the fibrinogen, although from these results it appears to give a similar precision in both instances. Considering that K_{av} is more easily measured than D_s , the equations of Ogston *et al.*³⁵ may well be useful in obtaining an estimate of D_s .

CONCLUSION

Diffusion coefficients of proteins inside a gel-filtration medium may be determined with fair accuracy by comparison of experimental and theoretical breakthrough curves, using the area A under the curves up to $t^* = 1$ (*i.e.*, holdback) as a matching parameter. Provided that the flow is sufficiently rapid, and that the stationary phase has a high equilibrium capacity for the protein, A will be large, and resistance to mass transfer through the mobile phase to the particle surface and dispersion due to non-uniformity of flow in the mobile phase will be secondary effects for which corrections can be made. The method of introducing the protein solution described here enables dispersion in the space at the top of the column to be minimized. Graphs are presented that enable the method to be applied without the need to compute the breakthrough curves again. The diffusion coefficients determined for porcine γ -globulin and porcine fibrinogen in Sepharose CL-4B of 11.2 and 3.6 $\mu\text{m}^2/\text{s}$ respectively, are about half those calculated on the basis of the equations of Ogston *et al.*³⁵.

APPENDIX

Note on computations

The library routine C06LAF requires the user to write a subroutine to calculate the Laplace transform given a complex value of s . In Fortran, complex numbers may be manipulated directly without the need to separate real and imaginary parts. It is important when using this library routine to know the approximate maximum value of

the inverse transform y . For this reason, in contrast to the inversion method of Chen and Hsu⁵, it is better to calculate the response to a step function, so that $y \leq 1$, rather than an impulse function, even though the impulse function involves a simpler transform. The routine was used to calculate y at 0.02 intervals of t^* in three ranges, 0.02–0.18, 0.20–1.00 and 1.02–2.00. The parameters TFAC and ALPHAB were both set to 1.0. The maximum number of terms to be used in the Fourier series approximation of the inverse transform was set to 50; usually about 20 terms were required. An accuracy of 1% was specified for y . At a few values of t^* , an error in y of greater than 1% was reported by the routine, but this did not contribute a significant error to A following the integration (eqn. 9) between $t^* = 0$ and 1 using Simpson's rule.

In the cases where $D_L/uL \neq 0$, y could be positive at negative times, and it was therefore necessary to shift the Laplace transform one unit along the time axis in order to avoid the problem of having to invert the transform at negative times. The integration to find A was then performed between $t^* = -0.3$ and 1.

ACKNOWLEDGEMENTS

I thank Dr. B. J. Bellhouse for his advice. Also, I am much indebted to Mrs. M. Unarska for many useful suggestions. I thank the Wolfson Foundation for financial support.

SYMBOLS

A	area beneath breakthrough curve
B	dimensionless constant in eqn. 10
c	concentration of protein, mg/cm ³
c_m	concentration in mobile phase
c_s	concentration in stationary phase
c_{in}	concentration at inlet of column
c_{out}	concentration at outlet of column
c_0	initial concentration in mobile phase
D_L	coefficient of longitudinal dispersion in the mobile phase
D_m	diffusion coefficient in mobile phase
D_s	diffusion coefficient in stationary phase
D_0	diffusion coefficient in free solution
D^*	$D_s V_a / R^2 Q$, non-dimensionalized diffusion coefficient.
h	reduced theoretical plate height
k	surface mass-transfer coefficient
K_{av}	V_a / V_s , partition coefficient
L	length of column
\mathcal{L}^{-1}	inverse Laplace transform
Q	discharge
r	radial coordinate inside spherical particles
R	radius of spherical particle
\bar{R}	mean radius giving equivalent surface area/volume
s	Laplace transform variable
S	surface area per unit volume of stationary phase

Sh	Sherwood number, Rk/D_m
t	time
t^*	$[V(t) - V_m]/V_a$, non-dimensionalized time
u	QL/V_m , average velocity, based on volume of mobile phase
v_f	volume fraction of fibres in the stationary phase
V	volume collected at outlet
V_a	partial volume of stationary phase accessible to the protein molecules
V_m	volume of mobile phase
V_s	volume of stationary phase
V_t	total volume of column
x	coordinate measured along column axis from inlet
y	$(c_{out} - c_0)/(c_{in} - c_0)$, non-dimensionalized form of concentration at outlet
α	$D_s K_{av}/kR$, surface mass-transfer resistance parameter
φ	function of s in eqn. 8
γ	$(1 - V_m/V_t)^{1/3}$, geometric parameter of Pfeffer's model
λ	dimensionless parameter of the model of Horváth and Lin
v	reduced velocity $2Ru/D_m$
σ	standard deviation of a chromatographic peak on volume axis
ω	dimensionless parameter of the model of Horváth and Lin.

REFERENCES

- 1 J. B. Rosen, *J. Chem. Phys.*, 10 (1952) 387.
- 2 J. B. Rosen, *Ind. Eng. Chem. Eng. Des. Process Dev.*, 46 (1954) 1590.
- 3 A. Rasmuson and I. Neretnieks, *AIChE J.*, 26 (1980) 686.
- 4 A. Rasmuson, *AIChE J.*, 31 (1985) 518.
- 5 T.-L. Chen and J. T. Hsu, *AIChE J.*, 33 (1987) 138.
- 6 R. E. Babcock, D. W. Green and R. H. Perry, *AIChE J.*, 5 (1966) 922.
- 7 A. Rasmuson, *Chem. Eng. Sci.*, 40 (1985) 621.
- 8 A. Rasmuson, *Chem. Eng. Sci.*, 40 (1985) 1115.
- 9 S. Brandt, R. A. Goffe, S. B. Kessler, J. L. O'Connor and S. E. Zale, *Bio/Technology*, 6 (1988) 779.
- 10 E. Kucera, *J. Chromatogr.*, 19 (1965) 237.
- 11 J. Villiermaux, *Chem. Eng. Sci.*, 27 (1972) 1231.
- 12 C. J. O. R. Morris and P. Morris, *Separation Methods in Biochemistry*, Pitman, London, 2nd. ed., 1976.
- 13 H. De Lasa, J. Hazlett and O. M. Fuller, *Chem. Eng. Sci.*, 41 (1986) 1233.
- 14 J. R. Hays, W. C. Clements and T. R. Harris, *AIChE J.*, 13 (1967) 374.
- 15 S. K. Gangwal, R. R. Hudgins, A. W. Bryson and P. L. Silveston, *Can. J. Chem. Eng.*, 49 (1971) 113.
- 16 P. F. Diesler, Jr. and R. H. Wilhelm, *Ind. Eng. Chem.*, 45 (1953) 1219.
- 17 H. A. Boniface and D. M. Ruthven, *Chem. Eng. Sci.*, 40 (1985) 2053.
- 18 P. V. Dankwerts, *Chem. Eng. Sci.*, 2 (1953) 1.
- 19 *Gel Filtration—Theory and Practice*, Pharmacia, Uppsala, 1985.
- 20 T. C. Laurent, *Biochim. Biophys. Acta*, 136 (1967) 199.
- 21 B. Öbrink, *J. Chromatogr.*, 37 (1968) 329.
- 22 *NAG FORTRAN Library, Mark 13*, Vol. 1, The Numerical Algorithms Group, Oxford, 1988.
- 23 R. Pfeffer and J. Happel, *AIChE J.*, 10 (1964) 605.
- 24 R. Pfeffer, *Ind. Eng. Chem. Fundam.*, 3 (1964) 380.
- 25 J. J. van Deemter, F. J. Zuiderweg and A. Klinkenberg, *Chem. Eng. Sci.*, 5 (1956) 271.
- 26 J. C. Giddings, *Nature (London)*, 184 (1959) 357.
- 27 G. Taylor, *Proc. R. Soc. London, Ser. A*, 219 (1953) 186.
- 28 J. C. Giddings, *J. Chromatogr.*, 5 (1961) 61.
- 29 J. F. K. Huber, *J. Chromatogr. Sci.*, 7 (1969) 85.

- 30 J. N. Done and J. H. Knox, *J. Chromatogr. Sci.*, 10 (1972) 606.
- 31 Cs. Horváth and H. J. Lin, *J. Chromatogr.*, 126 (1976) 401.
- 32 O. Levenspiel, *Chemical Reaction Engineering*, Wiley, New York, 2nd ed., 1972.
- 33 P. Schneider and J. M. Smith, *AIChE J.*, 14 (1968) 762.
- 34 H. E. Schultze and J. F. Heremans, *Molecular Biology of Human Proteins*, Vol. 1, Elsevier, Amsterdam, 1966.
- 35 A. G. Ogston, B. N. Preston and J. D. Wells, *Proc. R. Soc. London, Ser. A*, 333 (1973) 297.